Optica Applicata, Vol. XXVIII, No. 4, 1998

Multicrucible technology of tailored optical fibers

JAN DOROSZ

Biaglass Co. and Białystok University of Technology, 15–139 Białystok, Poland.

RYSZARD ROMANIUK

Warsaw University of Technology, Institute of Electronics Fundamentals, ul. Nowowiejska 15/19, 00–665 Warszawa, Poland.

The work presents recent developments in optical fiber technology at the Research and Production Department of Fiber Optics (in short Fiber Optic Department – FOD) at Biaglass Co. The modified multi-crucible technology of optical fibers, called the MMC process throughout this work, was used to obtain several kinds of usable optical fibers for sensors and functional components of fiber microoptics. The MMC optical fibers were measured and their parameters presented.

1. Introduction

The modified multicrucible technology of optical fibers (MMC process) gives soft-glass filaments of broadly tailored propagation characteristics. Essentially, three basic kinds of optical fibers can be drawn by the MMC process. We consider here fibers which are difficult to be drawn by any other method:

– optical fibers of very complex refractive index profiles (RIPs),

– optical fibers with more than one single-mode or multimode cores in the common cladding (multicore),

– optical fibers made of nonstandard glasses, optimized for particular application (sensory and photonic functional device fibers).

This paper describes the MMC version of the process for obtaining multicore optical fibers. Basic optical and transmission properties of manufactured multicore optical fibers are presented. Specific measurement methods have been applied due to the presence of a few closely spaced cores in one cladding.

2. MMC technology of optical fibers

A double crucible (DC) configuration for fiber pulling from glass melts was shown in paper [1]. Two concentric crucibles, each with a nozzle, are configured with their axes in the vertical direction. The crucibles are filled with appropriate core and cladding glasses. Premelted glasses must be poured to be crucibles. Another method is to fill the crucibles with small pieces of glass and then melt the glass slowly,

allowing excess time for the glass to degasify. The molten glass flows out through crucible nozzles. The flow is governed by the Poiseuille equation. The ratio of core to cladding radii is determined by the simple expression

$$a_r/a_p = \sqrt{Q_r/Q_p}$$

$Q = \pi P r^4/8\eta l$, $Q(r,p)$ – volumetric flow of core and cladding glases, P – pressure difference across the nozzle, η – viscosity, r, l – radius and length of nozzle.

The DC method is also used for the manufacturing of graded index fibers. This is done by selecting an appropriate pair of glasses that allow mutual interdiffusion to occur. A suitable dopant for the core is the one which increases substantially the refractive index and is easily diffusible. The diffusion process occurs only in a confined region, where the core glass enters the molten cladding glass near the two nozzles. Both glasses, in molten state, flow together in that region during fiber pulling process. A simple diffusion equation of radial symmetry applies to this situation. The concentration of the diffusible ion (here from core to cladding) follows the dependence

$$N(r/a) = N_0 \int_0^\infty \exp(Dtu^2/a^2) J_0(ur/a) J_1(ur) \mathrm{d}u$$

where: N_0 – initial concentration, D – diffusion coefficient, t – transit time through nozzle region, a – radius of core, J – Bessel function. Normalized diffusion coefficient is defined as $d = Dt/a^2$. The value of d is related to the volumetric flow by the expression $d = D\pi l/Q_r$. This simplification assumes that the refractive index profile of DC fiber matches closely the α profile. Figure 1 presents exemplary experimental data for refractive index profiles obtained for DC fibers for different values of d parameter.

2.1. MMC process with N coaxial crucibles

The basic initial assumption for N crucibles process and resulting multilayered optical fiber is the condition for constant fiber proportion. Constant proportions means that we are looking for stationary solutions of glass flow equation. The individual fiber layer flows result from particular crucible, while the total flow is confined by the outermost crucible of the biggest nozzle diameter. The known dependences for the DC process can be generalized for a set of N coaxially arranged pile of crucibles, to obtain

$$H_n = \frac{\rho_{n+1}}{\rho_n} \frac{k_n}{k_{n+1}} \left[\frac{(m-n)k_{n+1} - 1}{(m-n)k_n - k_m} \right] H_{n+1}, \quad \text{for } n = 1, \ldots, m-2,$$

$$H_n = \frac{\rho_{n-1}}{\rho_n} \frac{k_n}{k_n - k_{n+1}} H_{n+1}, \quad \text{for } n = m-1,$$

where: $n = 1$ – core, $n = 2 \ldots m$ – successive layers of the fiber, $k_n = \pi R^4 \rho_n g/8 A_n \eta_n L_n$, H_n – initial height of the fluid glass in the n-th crucible $H_n = h_n(t = 0)$; the following inequality must hold for k_n: $(m-n)k_n > k_m$. The coef-

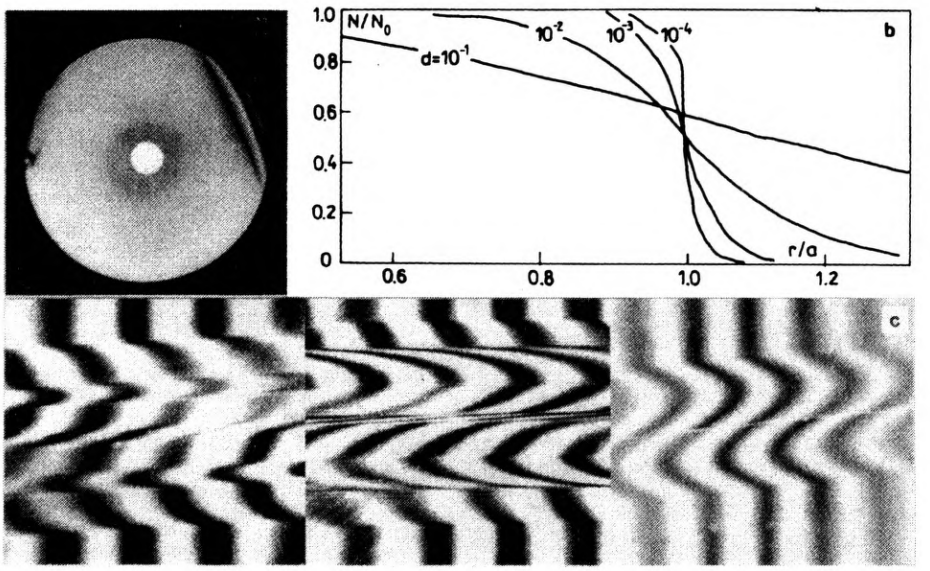

Fig. 1. Geometrical and optical characteristics of a standard DC fiber manufactured at FOD of Biaglass Co. **a** — microscopic photograph of a transverse cross-section (cleavage fracture) of exemplary DC optical fiber (dimensions: fiber external diameter 100 μm, core diameter 15 μm). **b** — normalized refractive index profiles of DC optical fibers manufactured at Biaglass Co. for various values of normalized diffusion coefficient $d = Dt/a^2$. The experimental curves agree quite well with theoretical predictions calculated with the aid of diffusion equation (within the accuracy of 3%). **c** — DC optical fiber in interference striated field. Successive microscopic photographs from left to right show fitting process of the refractive immersion environment to the refractive index of the fiber cladding. The fitting is perfect in the photo, which is the most right. The RIP of the fiber is determined from this photograph, with the aid of image processing software

ficients k_n are one of the most important parameters of the technological process. They depend considerably on temperature. Thus, temperature distribution along x- and z-axes of the furnace is of an essential importance.

The stationary solutions for one of the most practical setups of three crucibles are:

$$H_r = \frac{k_r(2k_{p1}-k_{p2})}{(2k_r-k_{p2})(k_{p1}-k_{p2})}\frac{\rho_{p2}}{\rho_r}H_{p2},$$

$$H_{p1} = \frac{k_{p1}}{k_{p1}-k_{p2}}\frac{\rho_{p2}}{\rho_{p1}}H_{p2}, \quad k_{p1} > k_{p2},$$

$$k_i = \pi R_i^4 g\rho_i/8A_i\eta_i L_i,$$

where: H — initial values for molten glass heights in crucibles, subscripts r, p_1, p_2 denote, respectively, r — core, p_1 — first cladding, p_2 — second cladding, p_3 — third cladding.

The stationary solutions for frequently used, in this laboratory, quadruple geometry setup are:

$$H_r = \frac{\rho_{p3}}{\rho_r}\frac{k_r(3k_{p1}-k_{p3})}{(2k_{p1}-k_{p3})(k_{p2}-k_{p3})(3k_r-k_{p3})}H_{p3},$$

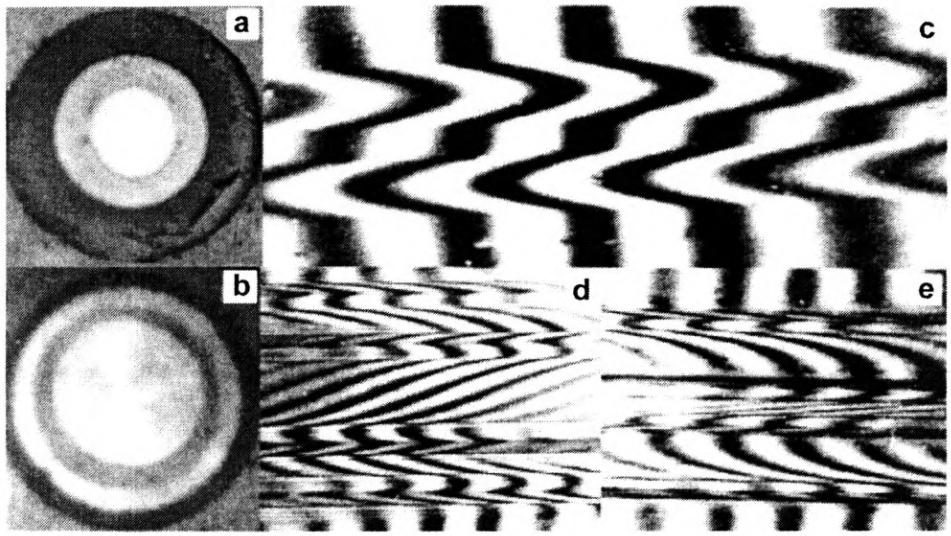

Fig. 2. Optical fibers manufactured during the MMC process with three (**a**) and four (**b**) coaxial crucibles, and images of the triple and quadruple crucible MMC optical fibers in striated field. Striated field image (**c**) of triple crucible fiber (upper) is perfectly immersion fitted. Striated field images of quadruple crucible MMC show the process of refractive immersion fitting. In the photo (**d**) the situation far from fitting is shown, while photo (**e**) shows the situation close to perfect fitting. RIPs of these fibers are presented in paper [2]

$$H_{p1} = \frac{\rho_{p2}}{\rho_r} \frac{k_{p1}(2k_{p2} - k_{p3})}{k_{p2}(2k_{p1} - k_{p3})} K_{p2},$$

$$H_{p2} = \frac{\rho_{p3}}{\rho_{p2}} \frac{k_{p2}}{k_{p2} - k_{p1}} H_{p3}.$$

The above dependences were used practically to pull several sample batches of MMC optical fibers of complex RIPs. The details of the MMC manufacturing process with N-coaxial crucibles were presented in [2].

Figure 2 presents practical application of the MMC process with N coaxial crucibles (see equations above) to manufacture three and four layered optical fibers of complex RIPs.

2.2. MMC process with N coaxial crucibles and modified (diaphragmed) nozzles

The DC and MMC processes can use hardware (crucibles and supporting frames between them) with glass flow modifying diaphragms. Since these diaphragms may influence essentially the glass flow conditions in between the crucibles and also the output resulting stream forming the possible fiber, the equations presented in the above Section have to be modified. We introduce this glass flow perturbation in the form of an intercrucible flow perturbation function F_p. This function, being an additional multiplying factor in the above equations, takes the form of a glass stream transmittance. Its arguments are: $F_p(\eta_i, \tau(x), S_i^c, E)$, where: η — viscosity of glass

from the i-th crucible, $\tau(x)$ – temperature distribution along the fiber forming and pulling path, S_i^c – surface shape function of diaphragm apertures between the i-th and $i+1$-th crucibles, E – experimental mofifying factor. The function F_p was applied with the above equations to calculate the conditions for stable fiber pulling of preset complex geometrical proportions (multi-layered, multicore and with tailored cores of complex shapes). Some of the optical fibers manufactured by means of this process were presented in [3], [4]. In practice, various MMC technology modifications were combined in one process. In particular, diaphragmed nozzles were combined with nozzle separation technique described below.

2.3. MMC process with internal crucible separation

There are several modifications of the classical DC process, leading to more complex optical fibers of tailored optical, sensory and propagation characteristics. One of the modifications, giving multicore optical fibers, is that with additional crucibles supplying separating glass layers. The crucible geometry in this kind of MMC is presented in Fig. 3. Internal and external crucibles 1 and 3 are connected with a permanent connecting pipe 4. This connection prevents the streams of glasses forming separate cores from gluing together, taking axial position, or changing their shape. The intermediate crucible 2 has the number of nozzles equal to the number of designed cores in the fiber. Crucibles 1 and 3 can be loaded with the same or different glasses. A central core, of different NA, is present in the fiber in the second case.

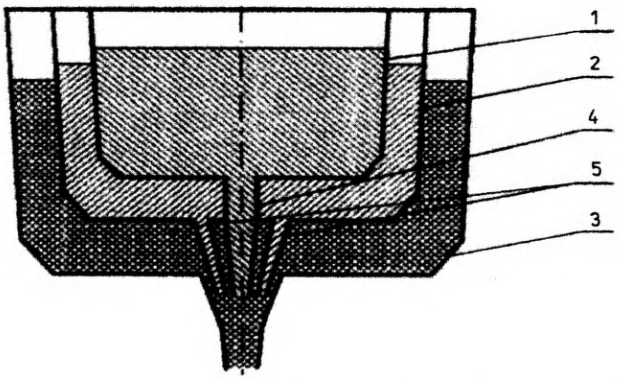

Fig. 3. Three crucible geometry for manufacturing MMC multicore optical fibers (internal crucible separation process): 1 – innermost crucible for axial core (contains core glass) or separation of off-axial cores (contains cladding glass), – 2 intermediate crucible with core glass and multiple nozzles, 3 – outermost crucible with cladding glass. While the nozzle diaphragming has been used in FOD since some time, the crucible separation technique is quite new. An obvious step in further development of the MMC process is combination of both fiber modifying techniques in a single process

The glass flow equations for these modifications of crucible geometry are modified as follows:

$$Q_1 = (\pi r_1^4 g/8\eta_1 L_1)(h_1\rho_1 - h_2\rho_2),$$

$$Q_1 = -A_1(\mathrm{d}h_1/\mathrm{d}t) = \pi R_1^2 v,$$
$$\mathrm{d}h_1/\mathrm{d}t = k_1(h_1 - \rho_3 h_3/\rho_1).$$

A similar set of equations is valid for other crucibles:

$$Q_2 = N(\pi r_2^4 g/8\eta_2 L_2)(h_2\rho_2 - h_3\rho_3), \quad Q_2 = -A_2(\mathrm{d}h_2/\mathrm{d}t) = N\pi R_2^2 v,$$
$$\mathrm{d}h_2/\mathrm{d}t = A_2 k_2(h_2 - \rho_3 h_3/\rho_1),$$
$$Q_3 = (\pi r_3^4 g h_3 \rho_3/8\eta_3 L_3), \quad Q_3 = -A_3\mathrm{d}h_3/\mathrm{d}t - A_1\mathrm{d}h_1/\mathrm{d}t - A_2\mathrm{d}h_2/\mathrm{d}t = \pi R_3^2 v,$$
$$A_3 k_3 h_3 = -(A_1\mathrm{d}h_1/\mathrm{d}t + A_2\mathrm{d}h_2/\mathrm{d}t + A_3\mathrm{d}h_3/\mathrm{d}t).$$

The coefficients k are:

$$k_1 = \pi r_1^4 g\rho_1/8\eta_1 L_1 A_1, \quad k_2 = N\pi r_2^4 g\rho_2/8\eta_2 L_2 A_2, \quad k_3 = \pi r_3^4 g\rho_3/8\eta_3 L_3 A_3,$$

k_i are characteristic coefficients of the MMC process. They are strong functions of temperature. Thus, to keep them stationary the process temperature has to be well stabilized, within 0.1 °C at the level of 1000 °C. The linear set of differential equations is

$$\mathrm{d}h_1/\mathrm{d}t = k_1(\rho_3 h_3/\rho_1 - h_1),$$
$$\mathrm{d}h_2/\mathrm{d}t = k_2(\rho_3 h_3/\rho_2 - h_2),$$
$$\mathrm{d}h_3/\mathrm{d}t = k_1 A_1 h_1/A_3 + k_2 A_2/A_3 - h_3(k_1\rho_3 A_1/\rho_1 A_3 + k_3).$$

With a solution for pulling velocity to obtain stationary fiber proportions:

$$v = (A_3 k_3 h_{3(0)}/\pi R_3^2)e^{xt}.$$

Using practically these dependences and numerical solutions several MMC (crucible separation) fiber samples were pulled. The fiber samples were chosen in such a way as to show the efficiency and flexibility of the MMC process in fiber characteristics design. The tailored MMC fiber samples were measured thoroughly using adapted optical apparatus used previously for standard optical fibers, either DC or PCS, or communication ones.

Table 1. High-purity glasses used for MMC fiber manufacturing (T_{soft} – softening temperature, α – coefficient of thermal expansion, n_p – characteristic refractive index)

Glass type	n_p	$\alpha \times 10^{-7}$/K	T_{soft} [°C]
F2	1.620	86	525
K7	1.511	82	610
BaLF5	1.567	81	575
SW1	1.522	85	585
SW7	1.613	83	585
SW8	1.515	90	610
BaLF1	1.563	71	570
BaLF2	1.548	81	580
SW4	1.523	93	590
BaF8	1.624	70	530

Table 2. Exemplary values of the MMC technological parameters during optical fiber production

Number of crucible W process parameter X	1	2	3
L [cm]	1	0.2	0.3
R [cm]	0.3	0.13	0.4
A [cm]	12.57	25.92	40.06
H [cm]	17.55	26.11	23
V [m/s]		0.196–0.220	

High-purity glasses were used for MMC optical fiber manufacturing. Their parameters are presented in Tabl. 1. The exemplary values of MMC process parameters are gathered in Tab. 2.

2.4. Basic types of MMC optical fibers manufactured by means of crucible separation process

Essentially two basic groups of MMC multicore optical fibers can be obtained with the aid of crucible separation process:

- optical fibers with off-axis cores of axial distribution,
- optical fibers with axial core and off-axis cores of axial distribution.

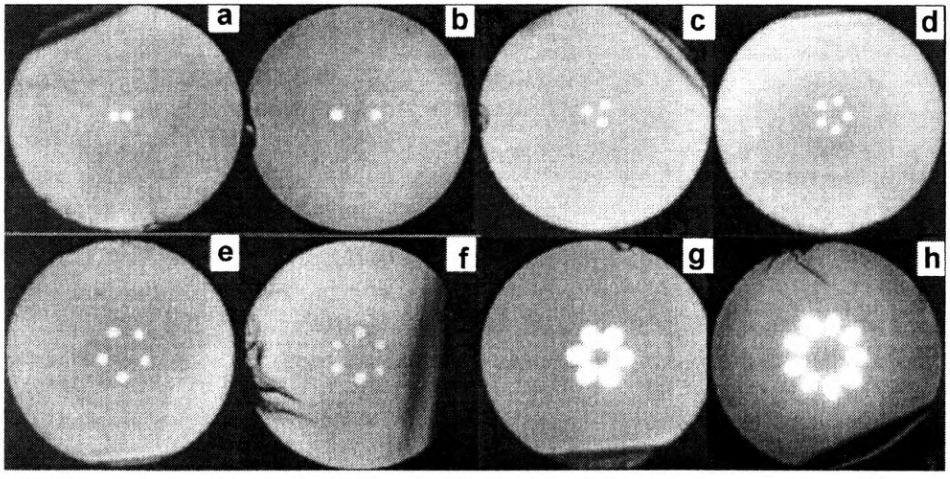

Fig. 4. MMC multicore optical fibers manufactured by internal crucible separation process. Axial crucible contains cladding glass: **a** – single-mode twin core optical fiber with strongly coupled cores (core separation smaller than core diameter), **b** – single-mode twin core optical fiber with practically noncoupled cores for nonperturbed fiber (the core coupling depends on fiber perturbation), **c** – single-mode triple core fiber with coupled cores, **d** – single-mode quintuple core optical fiber with coupled cores, **e** – single-mode quintuple core optical fiber with weakly-coupled cores, **f** – single-mode six-fold optical fiber with weakly-coupled cores, **g** – multimode optical fiber with 6-fold elliptical coupled core, **h** – multimode optical fiber with 9-fold elliptical coupled core. Exemplary fiber diameter may be around 60 μm, with core diameter 3–4 μm

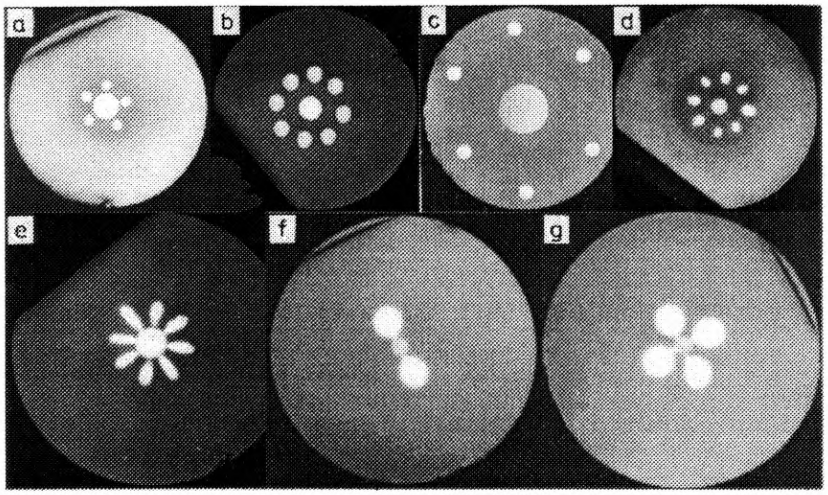

Fig. 5. MMC multicore optical fibers manufactured by crucible separation process. Axial crucible contains core glass: **a** — idea of a fiber with central multimode core and several single-mode cores around and coupled with the multimode one, **b** — circular geometry of multi-fold cores of the same dimensions, **c** — either single-mode or multimode cores placed very close to the outer cladding boundary, possibly for evanescent wave sensors, **d** — elliptical core multi-fold fiber, **f** — elliptical lobes adjacent to the central cylindrical core, **f** and **g** — idea of an-optical fiber with central single-mode core surrounded by several multimode cores of axial geometry, cores coupled

Some examples out of the two groups of fibers are presented in Figs. 4 and 5. These groups can be extended by combining crucible separation with nozzle diaphragming in a single MMC process.

2.4.1. Homo-core optical fibers

The optical fibers of multiple cores of exactly the same properties, like the ones presented in Fig. 4, are called homo-core fibers. Most of them are manufactured with the aid of a crucible separation process when the innermost crucible is filled with cladding glass. Homo-core fibers can also be manufactured during the process with the innermost crucible filled with core glass. The central core has to possess exactly the same properties as the off-axis cores.

2.4.2. Hetero-core optical fibers

The crucible separation MMC process makes it possible to manufacture (within the above two basic groups) not only homo-core optical fibers but also hetero-core ones. The hetero-core MMC optical fibers have at least two cores of different optical, physical, propagation, and other characteristics. Most of the fibers presented in Fig. 5 (the innermost crucible of the MMC process filled with the core glass) are hetero-core ones. We have investigated initially the simplest solutions for such MMC optical fibers:

— optical fibers with two or more circular cores of different diameters $d_{r_i} \neq d_{r_{i+j}}$,

– optical fibers of two or more circular or elliptical cores of the same diameters but different numerical apertures $NA_{r_i} \neq NA_{r_{i+j}}$.

Some examples out of the two groups of hetero-core optical fibers are presented, with some of their optical characteristics, in Figs. 11, 12, and 13. Hetero-core optical fibers have potentially very interesting applications as sensing fibers. The differential core sensitivity to eternal reactions can be utilized in these sensors. The fiber can work as a multi-wavelength dispersive element.

To manufacture some kinds of hetero-core MMC optical fibers (for example, having cores with different numerical apertures and different dispersion characteristics) the internal core crucible (the second one in Fig. 3) is divided to $N+1$ parts, where N is the designed number of cores in the fiber. The most inner, central crucible contains separating glass shifting the cores off the axis towards fiber circumference. A precise magnitude of this shift can be designed through the choice of the inner crucible nozzle diameter and shape, and viscosity characteristics of separating cladding glass.

The most important parameters of the MMC process for multi-NA-core optical fiber are:

– centricity of the divided core crucible against the cladding crucible and separating crucible,

– considerable differences in viscosities of glasssses of essentially different refractive indices.

The first problem is solved through the application of specially designed construction frame support for crucibles, which self-centers them. This self-centering ability of the support is enhanced by the possibility of fine tuning of the setup of crucible pile before permanent welding. The centricity of the crucible pile can be checked with laser equipment prior to using a particular setup in the furnace. The basic tolerance for nozzle spouts distribution is 10 μm.

The second problem is pretty complex and has no simple solution. The most obvious solution is experimental synthesis of own unique low-loss glasses for the hetero-NA optical fiber of particular design. These glasses should possess in pairs very similar thermal characteristics with possibly the most different refractive properties. Figures 11–13 present two and three core MMC optical fibers of different core dimensions and different values of numerical apertures of the cores.

2.4.3. HB optical fibers

A group of very interesting polarizing optical fibers can be manufactured with the aid of the MMC process. In particular, the stress-applying agents can be designed very precisely, in terms of their shapes, mechanical and thermal expansion properties. This leads to the rare and very difficult to obtain, via different technological processes, possibility to design very precisely the stress distribution inside the polarizing fiber. The stress distribution around the guiding single-mode core is of essential importance for the fiber polarization preserving characteristics, like beating length, perpendicular polarized mode suppression, *etc.* Some of the HB MMC optical fibers were persented in [3], [4], and some are subject of investigation in Fig. 14.

At first sight, some of the fiber designs may seem quite strange. This work shows, however, the potential power of the MMC technology to tailor the optical fiber according to the designer's wish. Some of the presented fibers have definitely strong application potential, and can be used either in switching, photonic functional devices like couplers, filters, or in sensors. Some of them were manufactured for pure research purposes to check the potential of the technology.

3. Measurements of MMC multicore optical fibers

One of the major problems with the tailored MMC optical fibers presented above is how to handle these fibers and measure them. They can be engineered to standard outside dimensions like 125 μm or so, but the cores will remain non-standard. The latter creates a lot of initial difficulties with optical power coupling, connecting, *etc.* We tried to overcome some of these difficulties using classical optical measurement methods [5].

3.1. MMC optical fiber measurement methods with interference differential contrast and negative phase contrast (striated fields)

Biolar PI microscope is equipped for measurements in interference homogeneous striated field. The interference is realized by three birefringent Wollastone prisms of different diffraction angles. The microscope tube prism gives striated field of large split r of image ($r = 32$ μm for a lens of $10\times$ magnification). The remaining two prisms invoke homogeneous interference area of small split ($r = 1.84$ μm for a lens with $10\times$ magnification) and big split ($r = 6.5$ μm for a lens with magnification $10\times$). The split originating from microscope tube birefringent prisms is constant and characteristic of these prisms. Adding a lens with rotary Wollastone birefringent prism to the optical system of PI microsope allows the split to be changed fluently, by rotating this lens against the optical axis. The relative position of all prisms involved (tube and lens) is neutral for rotation angles equal to $\gamma = 45°, 135°, 225°, 315°$. The wave split, in these cases, originates only from tube prism.

Rotating the lens prism by the following angles: 0° or 360° and 180° one can obtain additive and subtractive location of prisms. The split is respectively maximum when $r_{max} = r_1 + r_2$ and minimum when $r_{min} = r_2 - r_1$, where r_1 and r_2 denote split contribution values from birefringent tube and lens prisms. The rotation angles equal to $\gamma = 90°, 270°$ are equivalent to crossed setting left- and right-rotated. The value of resulting split r, for crossed position, is equal to $\mathrm{sqrt}(r_1^2 + r_2^2)$. When the slit of condensor diaphragm is narrow enough and set perpendicularly to the resulting direction of the wave split, there appears effective interference in the image plane of Biolar PI microscope. The vibrations of the split waves (by the lens prism), when entering the tube prism, must be in agreement with the main cross-section of the latter prism. The wave leaving the polarizer has to vibrate in the plane, which creates an angle of 45° with the main cross-section of tube prism.

At neutral, subtractive and additive settings, the direction of setting the condensor slit should be parallel to the direction of straight lined striae from the background of

the field of vision. At crossed settings, the slit should be rotated by such an angle so as to fit it to a position perpendicular to the resulting split of the front of optical wave.

The maximal split of optical fiber images, which one can obtain at crossed setting of birefringent prisms (tube and lens), equals $500/\beta$ μm, where β is the lens magnification. The measurements performed in the interference striae field, at the aforementioned split, have this advantage that the chosen value can be measured twice. Once in an ordinary image, and the second time in extraordinary image, which gives better accuracy of measurement.

This kind of interference is, however, not very useful in all cases. It depends, for a particular interferometer, on the diameter of the optical fiber measured and its core, on the number of cores and their distribution in the fiber. At high density of cores, the interference image gets non-readable, especially for regions close to fiber axis. In such cases the same interference microscope may be used but switched for differential interference.

Differential interference is a particular case of interference with double image. It is obtained as a result of slight transverse splitting of optical wave transmitted through the tested object. The difference in optical path-lengths Λ, in differential interference image, between ordinary and extraordinary waves does not express directly the difference of optical paths δ in the object, but a gradient of this difference $\mathrm{d}\delta/\mathrm{d}y$ in the direction r of the splitting of interference waves. The value of this split is of the same order as is the lens resolution in comparison with the diameter of the object. This property is described by the simple relation: $\Lambda = r\mathrm{d}\delta/\mathrm{d}y$.

The differential interference contrast in striated field can be obtained by subtractive setting of birefringent tube prism against the lens prism. Dense distribution of strips is a result of this and small resulting split of image.

At subtractive position of both prisms, the split of interfering waves takes place in the direction of optical fiber axis, which is set perpendicularly to the direction of striae in the background. Interference image, for anisotropic fibers, appears in the form of straight-line striae shifted in the area of fiber. This shift is a sum resulting from ordinary and extraordinary waves. For isotropic fibers, the shift is not observable or, in other words, it is equal to zero. In order to obtain differential image in the striated field, useful for further investigation and evaluation, it is necessary to use a compensator which would allow a continuous fluent change of direction and value of the image split. The other way out is to place the fiber at a very small angle to the striated field visible in the background. The interference image, created in this way, is characterized by the symmetric shifts of striae. The shift has opposite sign on both sides of optical fiber axis. The shift is zero exactly on the fiber axis, measured against striae chosen as a reference one. A characteristic feature of this kind of interference is zeroing of differential optical pathways on the fiber axis. The feature facilitates considerably identification of the order of striae shifted in optical fiber.

3.2. Measurements of striae shift in differential interference image of MMC optical fibers

The exemplary differential interference measurements were done on several kinds of

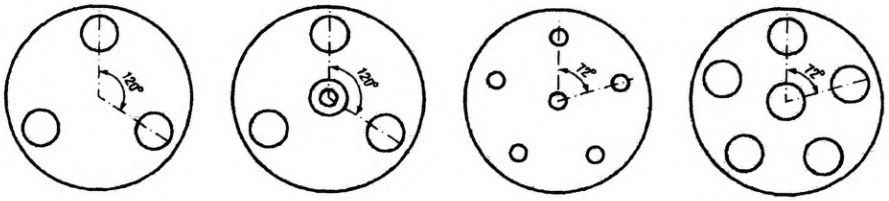

Fig. 6. Schematic transverse cross-sections of multicore MMC optical fibers under interferometric differential measurements. The fibers are further denoted as samples 1, 2, 3, 4

MMC optical fibers. Schematic cross-sections of four types of these fibers are presented in Fig. 6. These cross-sections are in agreement with real fibers presented in Figs. 4 and 5.

The data on striae shifts were read from interference images obtained by interference differential contrast method. A very small image split, of the order of single micrometers, which gives differential interferometry, allows us to observe quite readable interference images. These images are a base for geometrical shift measurements in chosen core of the fiber. The measurements were done for optical fibers placed in immersion environment of standard refractive index $n_m = 1.525$ and for wavelength $\lambda = 546$ nm. This particular wavelength was chosen with the aid of interference filter.

The shift for the striae of zeroth order, chosen as a measurement one, for triple-core optical fiber (sample 1) was assessed in all cores by rotation of the fiber by 120°. This measuring situation and the resulting striated field photographed from the microscope, for this fiber is presented in Fig. 7.

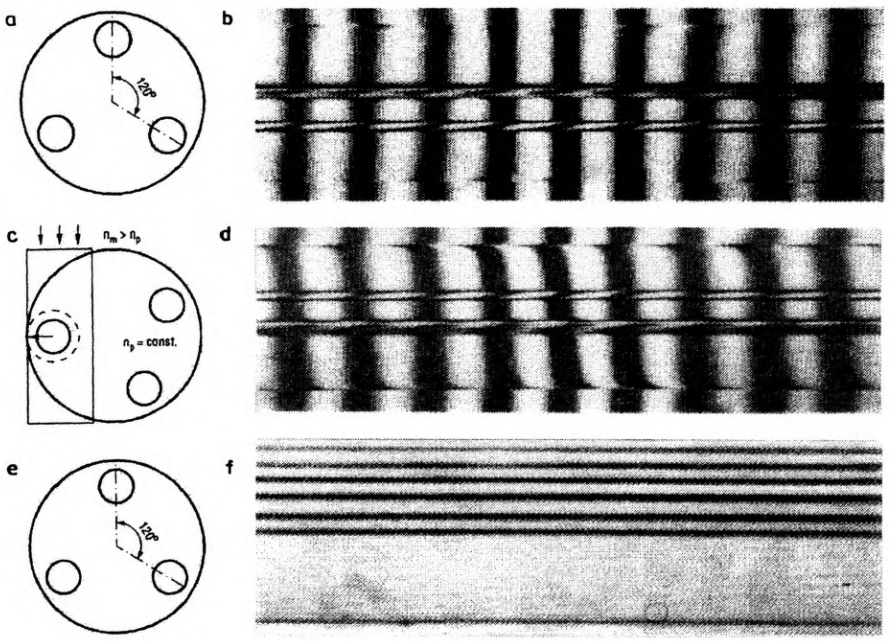

Fig. 7a–f

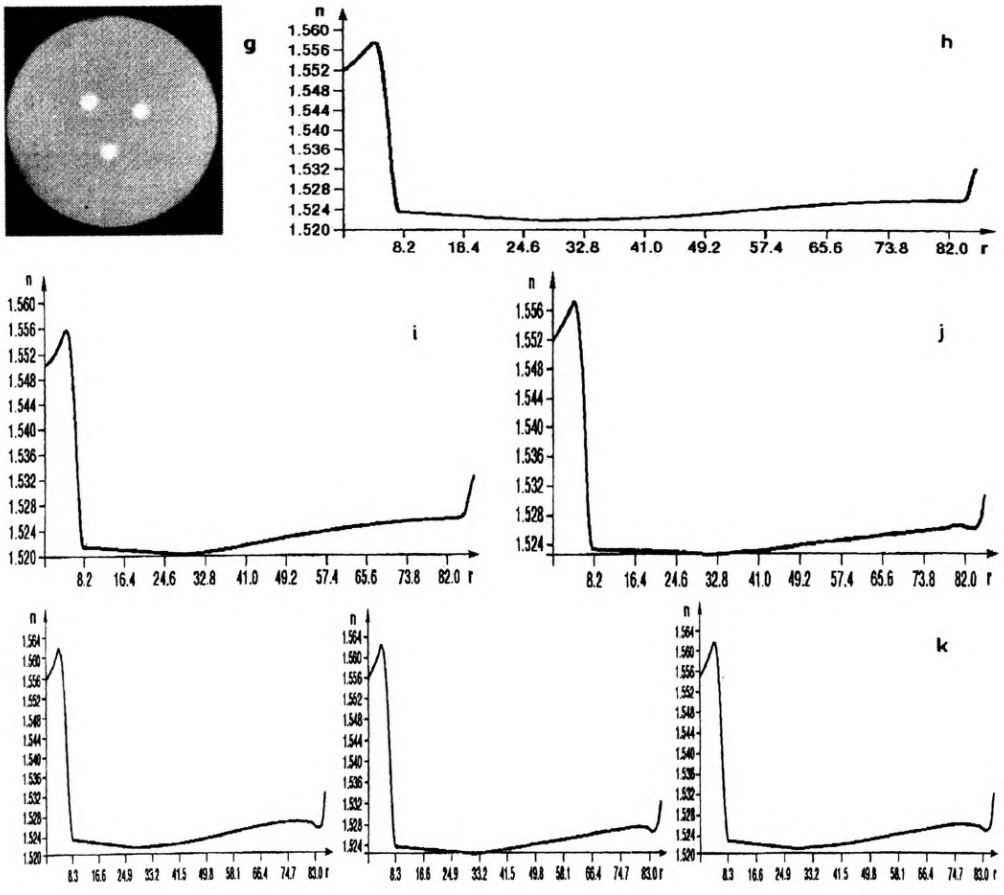

Fig. 7 g–k

Fig. 7. Schematic diagrams and optical and geometrical characteristics of triple core MMC optical fiber. **a** – schematic cross-section of fiber sample 1 with interference data collection for the whole fiber, **b** – differential interference image for $n_m = n_p$, $\lambda = 546$ μm, where n_m – immersion fluid refractive index and n_p – optical fiber cladding refractive index. Thus, in this case, the immersion environment neutralizes the cladding of the MMC multicore fiber. The differential interference images are used for determination of fiber refractive index profie. **c** – schematic cross-section of fiber sample 1 with marked area and direction of data collection on striae shift. **d** – differential interference image of triple-core optical fiber with data concerning one core chosen for measurements. **e** – schematic cross-section of fiber sample 1, and **f** – image of this fiber in microscopic negative phase contrast. The MNPC method is used for determination of fiber geometrical parameters. The individual core diameters in the fiber, measured by negative phse contrast were 15, 15 and 16.2 μm, respectively, with the accuracy in the range $\delta r = 0.250-0.066$ μm, depending on the magnification of the microscope objective. **g** – photograph of the measured triple core MMC optical fiber. **h** – RIP of photographed fiber (sample 1) for core 1 which is upper left on the photograph. Fiber axis measured in micrometers. **i** – RIP of the same fiber and for core 2 which is upper right on the photograph. **j** – RIP of the fiber for the third core 3 (lower). **k** – RIPs of three cores of analogous fiber from another batch pulling for comparison of the stability of MMC multicore fiber parameters

The same was done in the case of fiber sample 2. The difference is that the fiber has a quite complicated, additional core-cladding, on-axis structure. Rotating the fiber by 120°, measurements were done for off-axis cores, which is presented in Fig. 8.

The optical fibers from samples 3 and 4 required rotation by approximately 72° to measure the shift of striae in off-axis cores. The results for sample 3 are presented in Fig. 9, and the results for sample 4 are presented in Fig. 10. The shift data acquisition started usually from the fiber axis, where the value of derivative dR/dy was equal to zero. This characteristic place is comparatively easy to find on the interference image. It is a crossing point of straight-line extension to any line from the striated field from the background (for example, for zeroth interference order line) with the same striae shifted in the observed optical fiber.

Somehow more difficult was the assessment of the shift for the on-axis located cores in these MMC optical fibers. But, on the other hand, one has to remember of zeroing the derivative and of the symmetry in distribution of the outside (off-axis) cores. Part of the central core is located in the central area of the differential

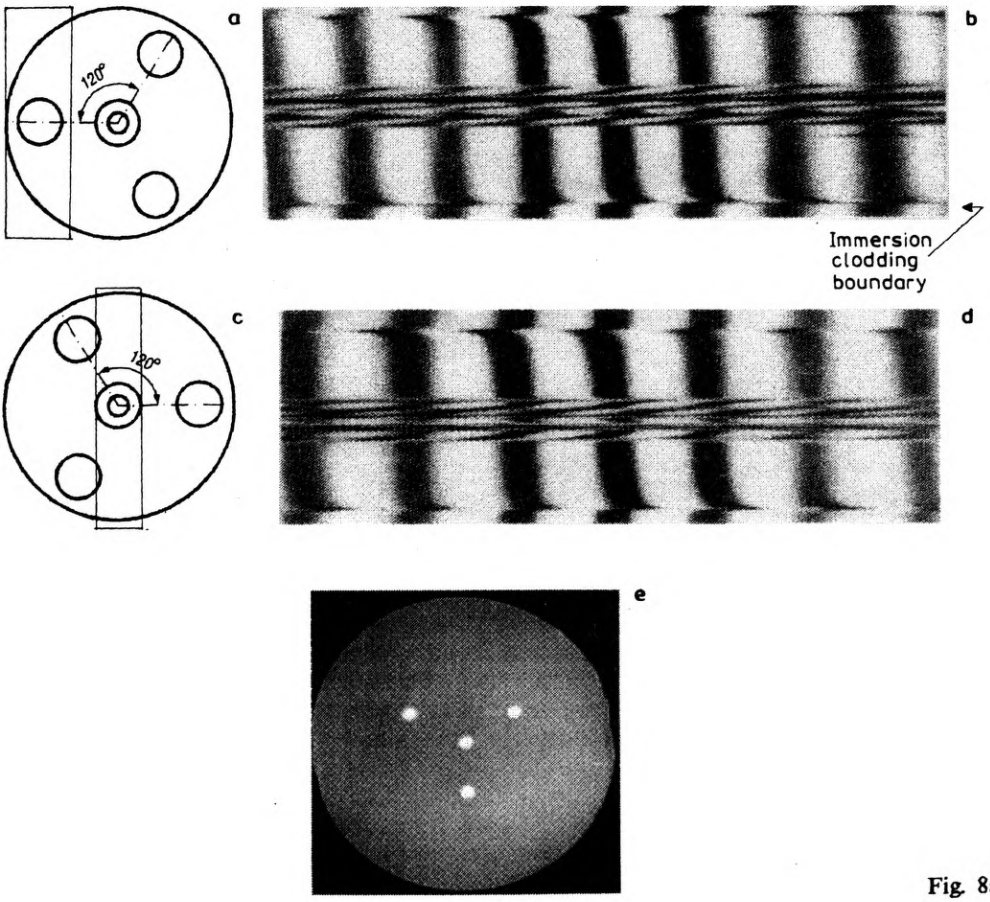

Fig. 8a–e

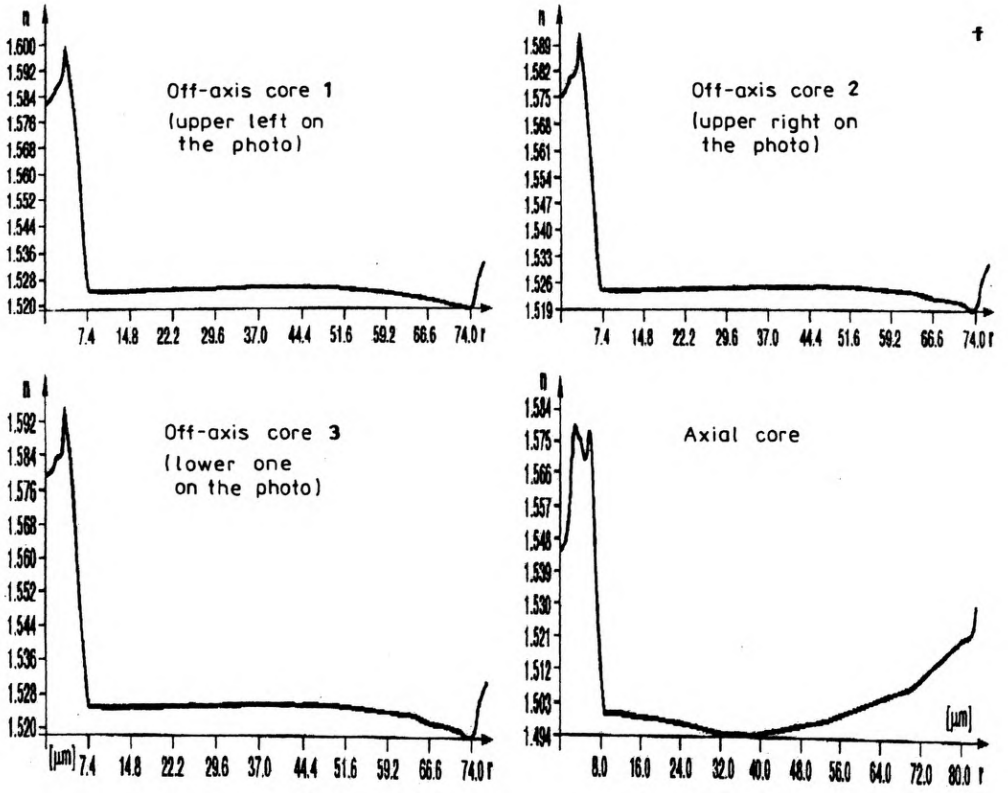

Fig. 8 f

Fig. 8. Schematic diagrams and optical and geometrical characteristics of quadrupole core MMC optical fiber sample 2. The fiber is similar to that one presented in Fig. 7 but has additional central core. The central core has thin extra cladding. **a** – schematic cross-section of fiber sample 2 with interference data collection for the area marked by rectangle, which includes a single off-axis core and fiber-immersion boundary, **b** – differential interference image for n_m close to n_p (actually n_m is slightly higher than n_p), and the situation from case **a**, **c** – schematic cross-section of fiber (sample 2) with interference data collection for the area marked by rectangle, which includes the central core, **d** – differential interference image for n_m close to n_p and the situation from case **c**, **e** – microscopic photograph of the measured quadruple core MMC optical fiber, **f** – refractive index profiles measured for all individual cores of the quadruple core MMC optical fiber from photograph **e**

interference image. The image of the central core is in the neighbourhood of superimposed images of the off-axis cores. These images are also presented in Figs. 8, 9 and 10.

Determination of striae shift in optical fiber samples 2, 3, and 4 for the central (on-axis) core starts from the fiber axis to the direction of its circumference with omitting the areas occupied by the off-axis cores. The shift measurement method assumes a few simplifications of fiber geometry: the fiber has perfect axial geometry, the fiber is perfectly circular, cores are circular and the refractive index in the core is constant $n_p = \text{const}$.

The character of changes of the cladding index n_p, in the optical fibers investigated, was measured by placing the fiber in an immersion fluid of the refractive index value n_m exactly equal to that of the cladding $n_m = n_p$. One of these measurements, for triple core MMC optical fiber, is presented in Fig. 6. It is seen that the straight-line striae from the background maintains its rectilinearity in the whole area of fiber cladding. This means that $n_p = \text{const}$. Further measurements of fiber RIPs exhibit also this feature.

The geometrical shifts in striated fields in MMC multicore optical fiber images were measured using standard graphical analysis software. The analyzed images were fed to appropriate image analysis environment and the shift was measured either manually, through a pointing device, or automatically using additional image analysis procedures with contrast enhancement.

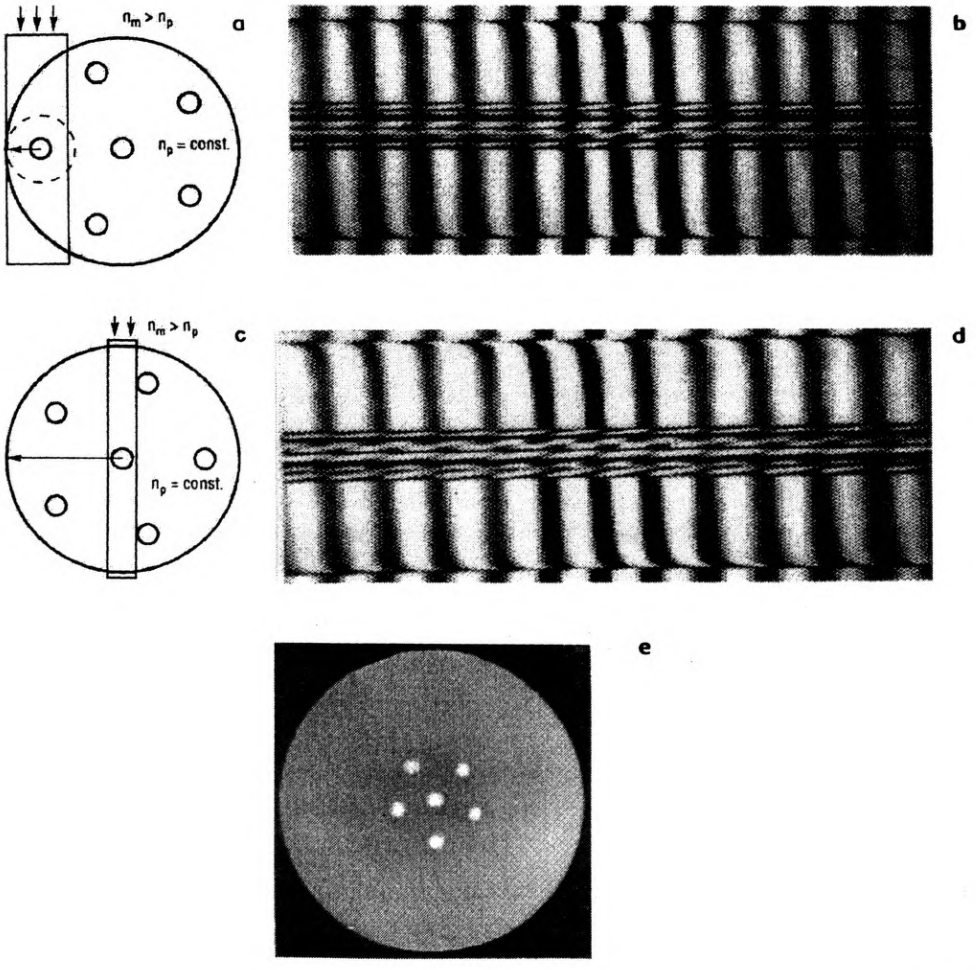

Fig. 9a–e

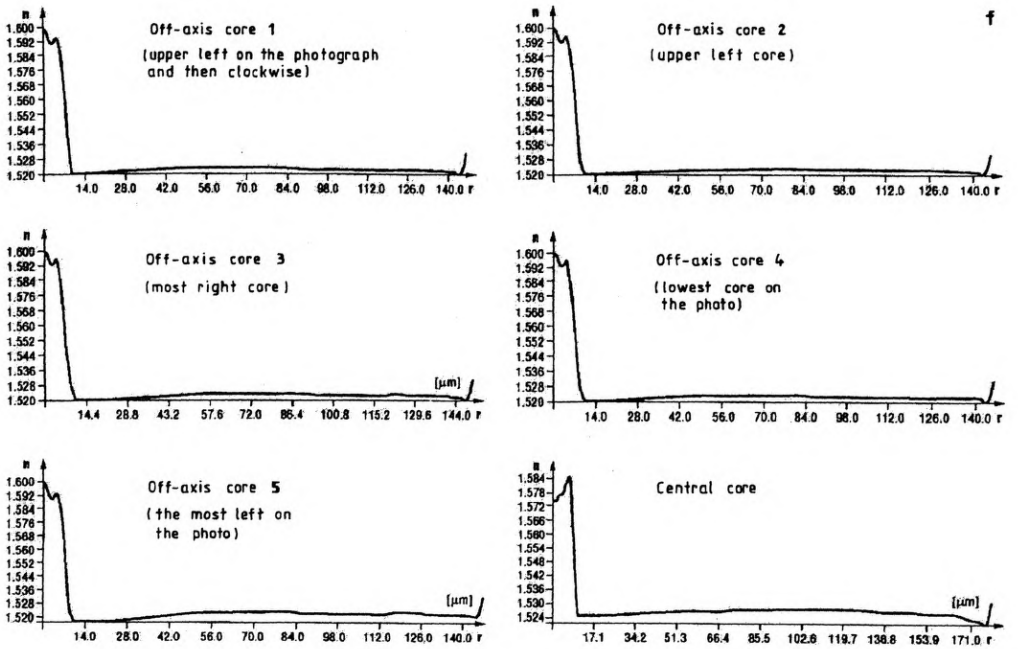

Fig. 9f

Fig. 9. Schematic diagrams, optical and geometrical characteristics of six-fold core MMC optical fiber (sample 3). The fiber is similar to that one presented presented in Fig. 8, but has more off-axis cores. One core is on-axis and five off-axis. All off-axis cores are nearly identical to accuracy of technological method. Central core is only slightly thicker. **a** – schematic cross-section of fiber sample 3 with interference data collection for the area marked by rectangle, which includes a single off-axis core and fibre-immersion boundary, **b** – differential interference image of the fiber for $n_m > n_p$ and the situation for case **a**, **c** – schematic cross-section of fiber sample 3 with interference data collection from the area marked by rectangle, the rectangle includes the central core, slice of cladding and fibre-immersion boundary, **d** – differential interference image for $n_m > n_p$, fiber-immersion boundary is clearly visible, **e** – microscopic photograph of the measured sixfold core MMC optical fiber – sample 3, **f** – refractive index profiles measured for all individual cores of the six-fold core MMC optical fiber from photograph **e**

3.3. Determination of refractive index profiles of MMC multicore optical fibers

The refractive index profiles in the samples of optical fibers presented were determined by the differential interference method from striae shift dR/dy as a function of y measured from the fiber center. The output data for computer based measurements were: n_m – refractive index of immersion fluid surrounding the fiber during recording of striated field, D_{mp} – initial distance between striae in the image background. The refractive index profile was determined from striated field in accordance with the following equations:

$$n(u) = \exp\left[\frac{1}{\pi}\int_u^1 \frac{\varphi(y)\mathrm{d}y}{(y^2-u^2)^{1/2}}\right], \quad 0 \leqslant u \leqslant 1,$$

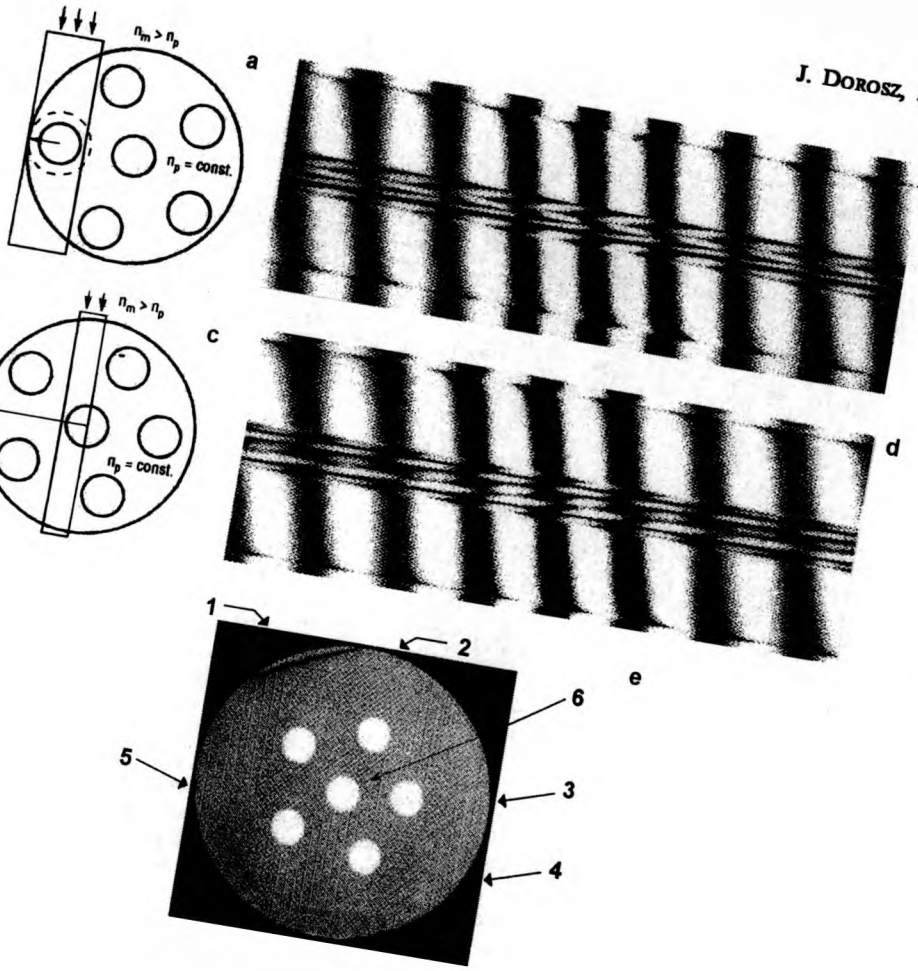
a
$n_m > n_p$
n_p = const.
b
c
$n_m > n_p$
n_p = const.
d
e
1
2
3
4
5
6

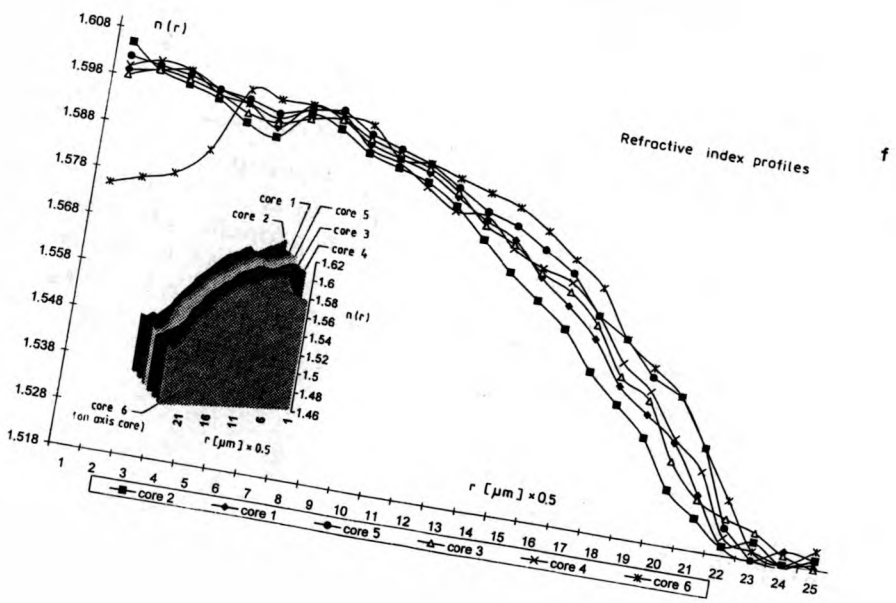
n (r)
Refractive index profiles
f
core 1
core 2
core 3
core 4
core 5
core 6
(on axis core)
r [μm] × 0.5
core 2
core 1
core 5
core 3
core 4
core 6

$$r = u/n(u), \quad \varphi(y) = -\arcsin\frac{\lambda}{D_{mp}}\frac{\mathrm{d}R(y)}{\mathrm{d}y},$$

where: φ – shift function, y – output coordinate.

The results of measurements and calculation for MMC fiber samples RIPs are presented in Figs. 6–10, adjacent to fiber pictures and views of their interferometric images.

Optical fibers from the first group of samples 1 are characterized by lower value of refractive index on the core axis. This lowering is equal to $\Delta n = 0.007$. The maximum value of refractive index in this sample group differed by the value $\Delta n = 0.005$. Similar in character are RIPs of optical fibers from sample group 2. The external cores in the fibers from this group have refractive dip on the core axis equal to $\Delta n = 0.008$, slightly bigger than for sample 1. Also, the maximum value of refractive index is bigger. Averaged maximum value was $n_{r_{max}} = 1.595$. The on-axis core of optical fibers from sample 1 has two layers. The maximum difference between refractive indices in the core is $\Delta n = 0.033$.

A considerable axial depletion of refractive index is exhibited by on-axis cores of optical fibers from sample group 3, which is equal to $\Delta n = 0.0111$, and from sample group 4, being equal to 0.0131. The off-axis cores of fibers from sample group 3 exhibit small local changes of refractive index, which are located not axially and equal $\Delta n = 0.008$. The off-axis cores of fibers from sample group 4 have only a slight axial refractive index depletion equal to $\Delta n = 0.004$. The changes of refractive index in the cladding of all fiber sample groups are comparatively very small. They do not exceed $\Delta n = 0.01$ on the average. Thus, we take an apologized assumption that the refractive index of the cladding is constant, $n_p = \text{const}$.

Analytical, and also simple visual, comparison of refractive index profiles $n(r)$ between the fibers in all samples reveals very small differences among them. This result says that the MMC process builds the individual cores (during pulling) of the multicore optical fiber quite homogeneously, and the diffusion processes (if any) are homogeneous. On the contrary, the sensory fiber designer may be interested in hetero-core fiber manufacturing of strictly engineered differential characteristics between cores.

◀ Fig. 10. Schematic diagrams, optical and geometrical characteristics of six-fold core MMC optical fiber (sample 4). The fiber is similar to that presented in Fig. 9 (sample 3), but has cores of greater diameter and thus is multimode. All cores are nearly identical to the accuracy of technological method. **a** – schematic cross-section of fiber sample 4 with interference data collection for the area marked by the rectangle, the area includes a single off-axis core, slice of cladding and fiber-immersion boundary, **b** – differential interference image of the fiber for $n_n > n_p$ and the situation from case **a**, **c** – schematic cross-section of fiber sample 4 with interference data collection from the area marked with a rectangle, the rectangle includes part of the central on-axsis core, a thin slice of the cladding and the fiber-immersion boundary, **d** – differential interference image for $n_m > n_p$ and the situation from case **c**, **e** – microscopic photograph of the measured six-fold core multimode MMC optical fiber (sample 4, fiber diameter around 180 μm, core diameters 21.5–22.5 μm), **f** – refractive index profiles measured for all individual cores of the six-fold core MMC optical fiber from photograph **e**. Inserted window shows a perspective view of the problem

3.4. Measurements of MMC multicore optical fiber dimensions and geometrical parameters

The MMC multicore optical fibers under investigation are mainly isotropic and, due to their shape, behave in transverse direction as cylindrical lenses. The diameters of core and cladding images observed in image plane of the microscope depend, to some extent, on the refractive index of the environment the fiber is submerged in (immersion). The lens like behaviour of the fiber (even a fiber of complex construction, either multicore of multi-layer) can be neutralized. This neutralization is needed during measurements of fiber geometrical parameters. When one measures the outside fiber diameter, the fiber can be immersed in a fluid of refractive index very close (the best, slightly smaller) than the fiber layer directly adjacent to the immersion.

The accuracy of determination of the optical path difference is considerably influenced by the diameter of the fiber core in micro-interferometric methods. This is of importance during the refractive index profile measurements. The shift of the interference striae, in refractively nonhomogeneous optical fiber, is determined for a strictly fixed distance y from the fiber axis. Determination of a particular measurement place in the fiber is connected with the knowledge of some geometrical parameters of the fiber, namely core and cladding diameters d_r and d_p.

Microscopic pictures of optical fibers were also obtained using the negative phase contrast method. Phase contrast microscope hardware of KFA type was used. In order to obtain a good contrast phase picture of an optical fiber, one has to set coaxially, and very precisely, a ring diaphragm against the corresponding phase ring of chosen lens. This diaphragm is in the turret disk of the condenser. The optical fiber has to be placed in the central view field of the microscope.

One has to know approximately the refractive index of the cladding, which is possible from the technological material data. The immersion environment is then prepared to match this approximate value of refractive index. The immersion environment has a slight refractive index gradient. The cladding of the optical fiber gets invisible exactly at the spot where $n_m = n_p$, or the index of cladding is equal to the index of immersion. In other words, the lightness of both objects gets the same: fiber core and background. Human eye estimates very precisely the differential lightness of adjacent objects or areas. Thus, the location of the place where $n_m = n_p$ is known quite precisely. The phase-contrast image of the fiber core is bright because always in fiber $n_p < n_r$ and simultaneously $n_m = n_p$. The condition of reliable measurement of optical fiber diameter is fulfilled. This measurement can be done either directly via the microscope eyepiece or with the aid of professional PC, image analysis software. The Biolar PI microscope has a specialized OK15MK binocular eyepiece for this purpose.

Table 3 shows the accuracy of determination of geometrical parameters (dimensions and shapes of core and cladding) of MMC optical fibers with the aid of microscopic negative phase contrast method, using the Biolar PI microscope (manufactured by PZO), for different settings of the optical system.

Table 3. Measurement accuracy for geometrical parameters of MMC optical fibers with the aid of negative phase contrast method and Biolar PI microscope

Nominal magnification of microscope lens [×]	10	20	30
Accuracy [±μm]	0.250	0.124	0.066
Nominal magnification of eyepiece [×]		15	

The geometrical parameters of optical fibers were determined, most frequently, at the magnificatin equal to 20×. The exemplary numerical values of these parameters for chosen fiber samples are gathered in Tab. 4. The MMC tailored optical fibers

Table 4. The exemplary measured values of geometrical parameters of optical fiber samples by the negative phase contrast method. The values in the table are in micrometers

Fiber sample Batch no. Presented as:	Core 1 Off-axis	Core 2 Off-axis	Core 3 Off-axis	Core 4 Off- or on-axis	Core 5 Off- or on-axis	Core 6 Off- or on-axis	Outer cladding
1; 1; photo	15.0	15.0	15.0	—	—	—	175.0
1; 2; RIP drawings	15.0	15.0	16.2	—	—	—	190.0
1; 3	16.2	16.2	16.2	—	—	—	190.0
2; 1; photo	14.0	14.1	14.0	14.0 on-axis	—	—	265.0
2; 2 RIP drawings	13.76	12.5	13.76	16.2 on-axis external region	4.92 on-axis central region	—	166.6
3; 1; photo	14.0	14.0	14.0	14.0	14.0	16.0	280.0
3; 2; RIP	18.8	18.8	18.8	18.8	18.8	18.8 on-axis	357.0
4; 1; photo	33.0	33.0	33.0	33.0	33.0	33.0 on-axis	285.0
4; 2; RIP	13.6	13.6	13.6	13.6	13.6	12.6 on-axis	205.4

manufactured can have dimensions ranging approximately between 10–500 μm (outside), with cores from single micrometers to occupying nearly the whole fiber, *i.e.*, with very thin outer cladding.

3.5. Measurements of material dispersion in MMC multicore optical fibers

Estimation of material dispersion in a multicomponent glass optical fiber is necessary for evaluation of fiber propagation properties. Multicomponent glasses

have individual values of material dispersion, which may differ substantially among sample glasses. This is unlike high silica optical fibers, where material dispersion is standardized and very well defined. A lot of practical applications of soft-glass optical fibers concern the usage of white light (or polychromatic light). In these applications, in some cases, the spectral dispersion of refractive index and, in particular, the dispersion of fiber numerical aperture may have a crucial meaning. Material dispersion is responsible, in digital signal transmission fibers, for pulse broadening, which is generally proportional to the second derivative of refractive index against the wavelength $\partial^2 n/\partial\lambda^2$. In signal transmission fibers, this effect is smaller than in multicomponent glass fibers.

Here, for the soft-glass optical fibers, the value of absolute difference between cladding and core indices is a strong function of wavelength: $\Delta n(\lambda) = n_r(\lambda) - n_p(\lambda)$

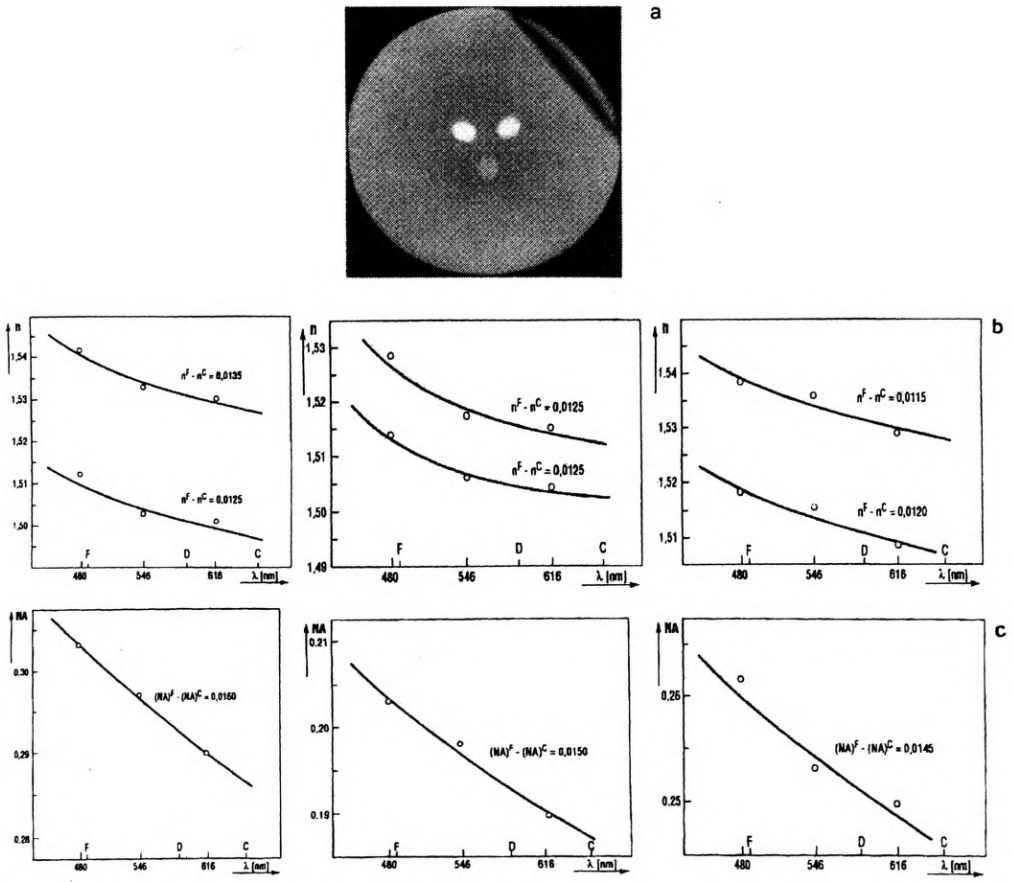

Fig. 11. Microscope photograph of cross-section of fiber sample 5 (**a**). The cores on the photograph are of different brightness. The core, which is upper left, has the biggest value of the $NA = NA_1 = 0.30$. Upper right core has $NA = NA_2 = 0.25$. The lowest core has $NA = NA_3 = 0.20$. Material dispersion characteristics of optical fiber (sample 5) for differential dispersion of refractive indices for all three cores and a single common cladding (**b**). Differential dispersion of numerical aperture for all three cores of fiber (**c**)

and in some cases (where wrong glass pairs are chosen) the basic propagation condition of optical fiber may be endangered. The propagating conditions in the fiber disappear when $\Delta n(\lambda_c = 0)$, where λ_c is a critical value of the wavelength for the chosen multicomponent pair of glasses (which are core and cladding of a fiber). This condition, only at first sight looks trivial, but in reality is not, as many sensor oriented multicomponent glass MMC fibers have very small value of numerical aperture. This aperture is subject to strong dispersion. Thus, the material spectral

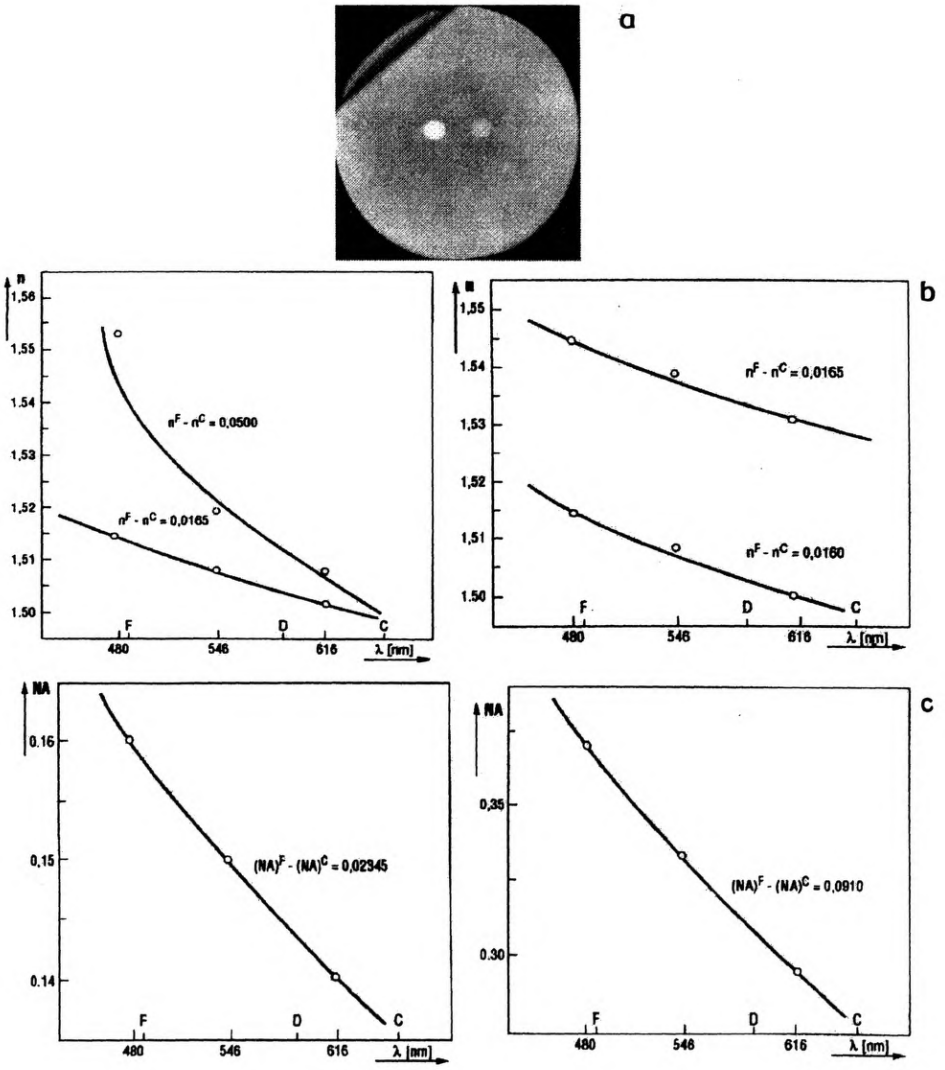

Fig. 12. Microscope photograph of cross-section of the fiber (sample 6), $NA_1 = 0.3$, $NA_2 = 0.15$ (**a**). Material dispersion characteristics of the optical fiber (sample 6). Differential dispersion of refractive indices for two elliptical cores and a common single cladding (**b**). Differential dispersion of numerical aperture for both cores of the fiber (**c**)

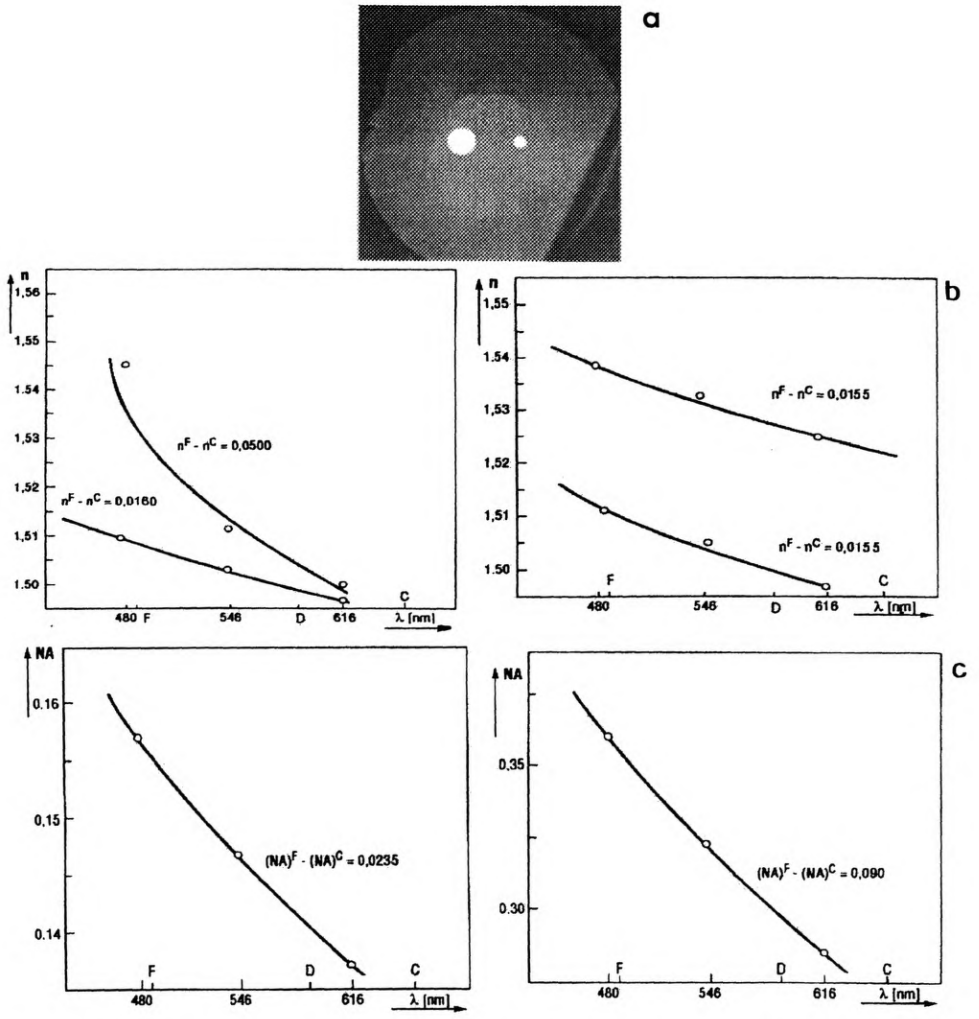

Fig. 13. Microscope photograph of cross-section of fiber sample 7 (**a**). This hetero-core optical fiber has cores of different diameters and numerical apertures. One of the interesting cases, from sensory point of view, is when the following condition is fulfilled for both cores $NA^1\varnothing^1 = NA^2\varnothing^2$ (where $\varnothing^i$ is *i*-th core diameter), or generally $NA^i\varnothing^i = NA^j\varnothing^j$. In the case of this fiber $NA\varnothing = 3$ μm. Material dispersion characteristics of optical fiber (sample 7): differential dispersion of refractive indices for two cores (**b**), differential dispersion of numerical aperture for both cores of the fiber (**c**)

dispersion characteristics of soft-glass optical fibers have to be assessed, researched and well known, prior to fiber application.

The material spectral dispersion of refractive indices and numerical apertures was investigated in three families of MMC optical fibers. They will be referred to as fiber samples 5, 6 and 7, in continuation of previous samples of the fibers investigated. These samples represent now the following fibers:

— sample 5: triple elliptical core optical fiber of different numerical apertures in each core,

– sample 6: double elliptical core optical fiber with different numerical apertures in each core,

– sample 7: double circular core optical fiber of cores with different diameters.

The fiber sample 5 represents a hetero-core optical fiber. The dimensions of elliptical cores in this fiber are nearly identical, within the accuracy of dimension measurements. The numerical apertures in the elliptical cores differ by a step of $\delta NA = 0.05$. In terms of the optical wave propagation, this difference is quite considerable. It means more in the case of a single-mode core than in the case of a multimode fiber. The cores on the photograph (Fig. 11) have different brightness. The numerical aperture increases clockwise from the upper left core with the biggest value of NA. All three cores were made of different low-loss fiberoptic grade glass. Thus, all cores have different material spectral dispersion. Therefore, they have different dispersion of numerical apertures. The cores have different sensitivities for external reactions. This one and similar fibers are prepared for optimized optical fiber sensory research, which will be carried out at FOD and at cooperating photonic laboratories.

The fiber sample 6 is a twin hetero-elliptical core optical fiber. Again, the cores have the same dimensions but considerably different numerical aperture. This is visible on the photograph (Fig. 12) by different brightnesses of particular cores. The numerical apertures of the cores in this fiber differ by the factor of two $NA^1 = 2(NA^2)$, which is quite large. Such a large value of multiplication factor requires careful choice of core glasses of quite different values of refractive indices but fitted thermally and mechanically. Frequently, this kind of task is connected with own specialized glass synthesis for this particular purpose. Glass sythesis research for sensory optical fibers seems to emerge as a separate interesting branch of material engineering.

A potentially very complex model of hetero-core optical fiber is sample 7, presented in Fig. 13. The fiber has, for example, two cores which differ in dimensions. The two cores can have different or identical optical parameters. This particular fiber has cores of different dimensions and different numerical apertures. The idea of a fiber of this kind may included, for example, a model of single-mode core coupled strongly with multimode one. Several different propagation or optical conditions may be fulfilled in such a fiber leading to important photonic sensing solutions. The fiber can have two single-mode cores with slightly different propagation characteristics. The differential characteristics can then be utilized for stable polarization maintenance of propagating wave, when the cores are strongly coupled, for signal switching or for sensory purposes, including interferometric ones.

The investigations of dispersive properties of optical fibers (samples 5, 6 and 7) were done with the aid of shearing microinterferometer and interference filters. Carl Zeiss Jena filters were used and Biolar PI interference microscope. The filters has the following nominal transmission wavelengths: $\lambda = 661, 546, 480$ μm. The RIPs were determined using transverse interference method with differential split of the front of optical wave. The spectral dispersion of refractive index in individual

cores and dispersion of the NA value was expressed by mean dispersion, assuming the following spectral standard lines: $F(\lambda = 486\ \mu m)$, $C(\lambda = 656\ \mu m)$.

Figures 11, 12 and 13 present refractive index dispersion in the cores and claddings of the fibers and spectral dispersion of the NA. The value of parameter $n^i_{F-C} = (n^F_i - n^C_i)$ in the cladding of fiber sample 5 is constant and equals 0.0125. The value of $n(F-C)$ in particular cores of fiber sample 5 diminishes continuously from the first to the third core, from $n^1(F-C) = 0.0135$, $n^2(F-C) = 0.0125$, $n^3(F-C) = 0.0115$. The mean dispersion of NA value $NA^i_{F-C} = [(NA_i)^F - (NA_i)^C]$ behaves similarly. This dispersion of refractive index in the cladding of fiber sample 6 equals $n^p(F-C) = 0.0160 \pm 0.0005$ and is constant. The dispersion in the first cladding is equal to $n^1(F-C) = 0.0500$. The dispersion in the second core is equal to $n^2(F-C) = 0.0165$. The dispersion of the numerical aperture NA is different in each core and equals $NA^1_{F-C} = 0.02345$ – for the first core, and $NA^2_{F-C} = 0.0910$ – for the second core.

It is to be assumed that the reasons for all these substantial changes in the measured dispersive parameters are diffusion processes, which take place during the process of MMC optical fiber pulling. These processes are, to some extent, similar to those which occur in single-core optical fibers. Here, however, unlike in the case of a single-core optical fiber, there are several sources of migrating glass ions. This may complicate the diffusion model, especially when the cores are separated only very closely from each other. The dispersion parameters for the fiber samples are gathered in Tab. 5.

Table 5. Material dispersion parameters of chosen samples of MMC optical fibers

Fiber parameter→ Fiber sample Region of fiber↓	Numerical aperture	$n_F - n_C$	$NA^F - NA^C$
5; cladding	–	0.0125	–
5; core 1	0.3	0.0135	0.160
5; core 2	0.25	0.0125	0.150
5; core 3	0.2	0.0115	0.145
6; cladding	–	0.0160	–
6; core 1	0.3	0.050	0.02345
6; core 2	0.15	0.0165	0.09100
7; cladding	–	0.0160	–
7; core 1	0.30	0.050	0.0235
7; core 2	0.15	0.155	0.090

3.6. Measurements of polarization properties of MMC multicore optical fibers

The birefringence in optical fibers is introduced during the technological process. This concerns mainly communication fibers and the CVD process. Two basic ways of introducing birefringence in the optical fiber are: circular geometry disturbance of the fiber and the core, and freezing of internal anisotropic stress around the core. The third way is to propagate the wave in a fiber with two (or more) strongly coupled

cores (single-mode). Generally speaking, the resulting fiber birefringence is a sum of shape and stress components. The birefringence affects the state of polarization of lightwave propagating in the fiber. The simplest example of a birefringent optical fiber is the one with an elliptical core. This type is called internal geometric birefringence. Stress birefringence is induced in a fiber by one or two stress agents of different shapes, which are embedded in the fiber close to the core.

The MMC process with crucible separation enables manufacturing of a few groups of basic solutions to (highly) birefringent optical fibers (referred frequently to as HB fibers). Some of the examples of such fibers (Panda, Bow tie, D *etc.*) were presented in [5]. During the MMC process with crucible separation, unlike in its previous usage, described in this paper, the innermost crucible is filled with core glass. The intermediate crucible is filled with glass, from which stress agents arepulled. The outermost crucible is, of course, the cladding. The MMC process in this case has a very rich collection of technological tools to design the HB fibers. In particular, the properties of the stress agents (dimensions, shapes, mechanical and thermal properties, closeness to the core *etc.*) can be extremely subtly tuned. Thus, the excess stress distribution in close vicinity of the fiber core can be precisely engineered. This, in turn, leads to introduction of strictly controlled birefringence to the fiber.

Using standard laboratory setup for observing optical Fourier transforms, the multicore MMC optical fibers were observed. Optical fibers of complex internal structure involving several cores, of different dimensions, different numerical apertures, *etc.*, have very complex optical Fourier transforms consisting of several tens of striae covering the whole transform image. In zero position, the transform totally covers the conoscopic cross. On the other hand, the Fourier transform obtained after rotating the complex multicore fiber by 90° barely covers only the parts of the conoscopic cross. The first Fourier transform is equivalent to complex, heterocore fiber position, where optical core of the biggest value of refractive index is positioned over the central on-axis core. As regards the second Fourier transform this core (the biggest one of the biggest dimensions and the biggest value of refractive index) is totally uncovered, and the rest of cores overlap partially.

Of a similar character are Fourier transforms of polarization maintaining MMC optical fibers. Figure 14 presents a couple of such Fourier transforms for soft-glass, MMC, polarization maintaining optical fibers, including Panda, D and twin elliptical core ones. The transforms are functions of fiber dimensions, positioning, refractive properties, *etc.* These fibers exhibit strong polarization properties. The last of the images shows the Fourier transform for six-core optical fiber. This fiber exactly was subject of previous investigations (fiber sample 3).

All multicore optical fibers create Fourier trasforms, which are more or less symmetrical, as was to be anticipated. They represent different geometrical constructions and optical properties. The Fourier transforms possess total, or slightly spaced, conoscopic cross, and are characterized by plenty of slim striae. The striae appear on the whole surface of the transform with bigger or smaller density.

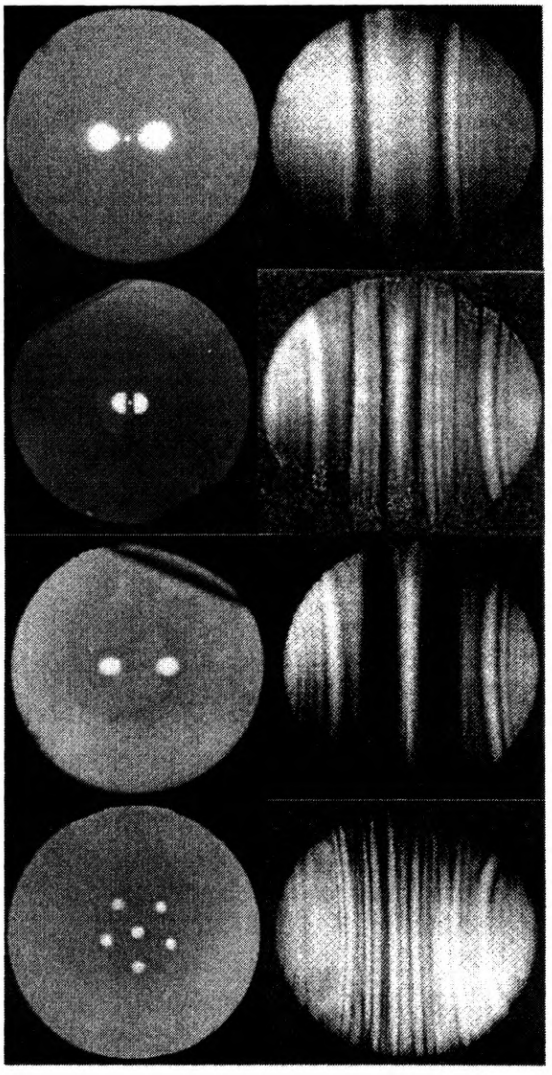

Fig. 14. Cross-section images of chosen MMC optical fibers manufactured with the aid of crucible separation process and their Fourier transform images. HB single-mode Panda fiber (a), HB single-mode double D fiber (b), multimode twin elliptical core fiber with separated cores (c), multicore fiber (sample 3) which was the subject of previous investigation presented in Fig. 9e (d)

Multicore optical fibers have many Fourier transforms, which may be observed rotating the fibers in the object plane round their long axis. Two-core optical fibers have two characteristic Fourier transforms, which are transformed one into another through several intermediate stages. Three-core optical fibers possess three most characteristic Fourier transforms. From these transforms several characteristic features of the fiber can be read.

Optical Fourier transforms of fibers with five, six and more cores are a set of straight linear striated images. The width of these striae is increasing towards the centre of the image. The width of striae in the central part of the image depends on the dimensions of the cores located around the fiber axis.

The observed Fourier transforms reveal polarization properties of observed optical fibers. The fibers are birefringent in the direction transverse to its main axis and these polarization properties change with fiber rotation by 90°. The Fourier transform images enable subtle classification of manufactured optical fibers according to their polarization properties. The precise qualitative and quantitative evaluation of the Fourier transform interferograms is done using image analysis software.

4. Conclusions

The paper presents the possibilities of the modified crucible technology of optical fiber manufacturing. New solutions for soft glass optical fiber design are presented and practically checked. On the technological level, the research was connected with determination of:

– nozzle glass flow stability conditions for novel continuous MMC process fiber manufacturing with separated crucible,

– conditions for continuous MMC fiber manufacturing of stable dimensions during the whole process for multicrucible setup.

Novel solutions for technological equipment were designed, performed and practically applied. Process parameters, having the most crucial influence on the fiber properties were assessed and estimated quantitatively and qualitatively. Two main methods of MMC process for multicore optical fibers were investigated more closely:

– crucible nozzle diaphragming [3],

– internal crucible separation (presented in this work in more detail).

Quite new technological possibilities are expected through combining both methods in the future redesign of technological equipment.

Single-mode and multimode optical fibers with two up to nine cores were manufactured using these methods. The fibers were homo-core or hetero-core. Hetero-core fibers have more than two cores of different optical properties. Using several basic optical measurement techniques, some of the characteristics of MMC multicore optical fibers were measured and analyzed. In particular, the following parameters were measured: refractive index profiles, material dispersion, birefringence, *etc.*

Further research on the tailored single-mode and multimode soft-glass optical fibers depends, to a large extent, on potential applications of such fibers. The research group, which manufactured these fibers and made initial research on them, promotes their applications in the field of continuously and dynamically developing area of optical fibers sensor. Several model sensors with tailored fibers (and strictly utilizing the uniqueness of these fibers) were manufactured, such as: twin core

rotation and torque sensors, liquid level sensor, chemical sensors with opto-chemical interfaces, mechanical stress and bend sensors, *etc.* The results of these experiments will be published soon.

References

[1] DOROSZ J., Elektronika **23** (1982), 30 (in Polish).

[2] DOROSZ J., ROMANIUK R., *Optical fiber technology by triple and quadruple crucible methods*, [In] VI Int. Fiber Optics and Communications Conf. (IFOC'82), Los Angeles, August 1982, pp. 99–102.

[3] DOROSZ J., *Crucible technology of multicore optical fibers*, Research Dissertations of Technical University of Białystok (in Polish, contains English summary), Vol. 29 (1995).

[4] DOROSZ J., *Theoretical and practical problems of multicore fiber optic technology*, Research Dissertations of Technical University of Białystok (in Polish, contains Emglish summary), Vol. 41 (1997).

[5] BOŻYK M., *Transverse interference methods applied to optical fiber research. Development of optical fiber technology*, (in Polish), Program Report No. RRI 02, University of Maria Curie-Skłodowska, Lublin 1990.

Received October 19, 1998